Author Manuscript

Author Manuscript

Author Manuscript

Author Manuscript

HHS Public Access

Author manuscript

Arch Biochem Biophys. Author manuscript; available in PMC 2018 November 15.

Published in final edited form as:

Arch Biochem Biophys. 2017 November 15; 634: 38–46. doi:10.1016/j.abb.2017.09.017.

FUNCTIONAL SIGNIFICANCE OF C-TERMINAL MOBILE DOMAIN OF CARDIAC TROPONIN I

Nazanin Bohlooli Ghashghaee[a], **Bertrand C. W. Tanner**[b], and **Wen-Ji Dong**[a,b]

[a]The Gene and Linda Voiland School of Chemical Engineering and Bioengineering, Washington State University, Pullman, WA 99164, USA

[b]The Department of Integrative Physiology and Neuroscience, Washington State University, Pullman, WA 99164, USA

Abstract

Ca^{2+}-regulation of cardiac contractility is mediated through the troponin complex, which comprises three subunits: cTnC, cTnI, and cTnT. As intracellular [Ca^{2+}] increases, cTnI reduces its binding interactions with actin to primarily interact with cTnC, thereby enabling contraction. A portion of this regulatory switching involves the mobile domain of cTnI (cTnI-MD), the role of which in muscle contractility is still elusive. To study the functional significance of cTnI-MD, we engineered two cTnI constructs in which the MD was truncated to various extents: cTnI(1–167) and cTnI(1–193). These truncations were exchanged for endogenous cTnI in skinned rat papillary muscle fibers, and their influence on Ca^{2+}-activated contraction and cross-bridge cycling kinetics was assessed at short (1.9μm) and long (2.2μm) sarcomere lengths (SLs). Our results show that the cTnI(1–167) truncation diminished the SL-induced increase in Ca^{2+}-sensitivity of contraction, but not the SL-dependent increase in maximal tension, suggesting an uncoupling between the thin and thick filament contributions to length dependent activation. Compared to cTnI(WT), both truncations displayed greater Ca^{2+}-sensitivity and faster cross-bridge attachment rates at both SLs. Furthermore, cTnI(1–167) slowed MgADP release rate and enhanced cross-bridge binding. Our findings imply that cTnI-MD truncations affect the blocked-to closed-state transition(s) and destabilize the closed-state position of tropomyosin.

Keywords

Troponin; cardiac troponin I; length dependent activation; cross-bridge kinetics; mobile domain truncation

Corresponding author: Wen-Ji Dong, The Gene and Linda Voiland School of Chemical Engineering and Bioengineering, Washington State University, Pullman, WA 99164, USA. Tel: 509-335-5798, Fax: 509-335-4806, wdong@vetmed.wsu.edu.

Publisher's Disclaimer: This is a PDF file of an unedited manuscript that has been accepted for publication. As a service to our customers we are providing this early version of the manuscript. The manuscript will undergo copyediting, typesetting, and review of the resulting proof before it is published in its final citable form. Please note that during the production process errors may be discovered which could affect the content, and all legal disclaimers that apply to the journal pertain.

Disclosures

No conflicts of interest, financial or otherwise, are declared by the author(s).

Author Manuscript Author Manuscript Author Manuscript Author Manuscript

1. Introduction

Contraction of vertebrate striated (skeletal and cardiac) muscle is Ca^{2+}-regulated by the troponin complex through interactions with the actin filament and tropomyosin [1]. The troponin complex consists of three subunits: troponin C (TnC), the Ca^{2+}-binding subunit; troponin I (TnI), the actomyosin MgATPase-inhibitory subunit; and troponin T (TnT), the tropomyosin-binding subunit [2–4]. During diastole, cTnI interacts tightly with actin and tropomyosin, and as a result, cTnI-tropomyosin prevents the actomyosin interaction through steric blocking of myosin binding sites on actin [5, 6]. During systole, Ca^{2+} binding to the N-domain of cTnC causes a partial exposure of the hydrophobic cleft of the N-domain of cTnC [7, 8], followed by the interaction between the hydrophobic cleft of cTnC and the switch region of cTnI [1, 4, 9–11]. This latter interaction drags both the inhibitory region and mobile domain of cTnI (cTnI-MD) toward cTnC as they release from actin [7, 8, 10, 12–16]. These movements of the C-terminus of cTnI alter the orientation and flexibility of troponin and tropomyosin relative to the actin filament [17], and cause tropomyosin to move on the actin surface from the blocked-state toward the closed-state [18], thereby permitting strong cross-bridge binding with actin [6, 18–22].

Beside Ca^{2+} regulation, cross-bridge formation is spatially-regulated by sarcomere length (SL) [1, 4, 23]. Length dependent activation (LDA) of cardiac muscle is an outstanding feature of the heart which is associated with increased tension development and increased Ca^{2+}-sensitivity of myofilament activation. Consequently, the number of potential cross-bridges that become available to generate force during a heartbeat is influenced by both Ca^{2+}-regulation and SL. However, the underlying mechanism of LDA is still unknown. Different characteristics of the myofilaments contribute to LDA, such as the inter-filament lattice spacing [24–26], the distinctive structural changes in thick and thin filaments [27, 28], the orientation and number of cross-bridges [29–31], titin-based passive tension [32–37], and the increase in positive feedback on myocardial contractile regulation [38–40]. Our previous studies have shown that Ca^{2+}-induced opening of the N-domain of cTnC [40], and Ca^{2+}-induced movement of C-terminus of cTnI [41] are both SL- and cross-bridge-dependent. These results suggest an interplay between the thin filament- and thick filament-based regulatory mechanisms of LDA [27].

Among thin filament proteins, cTnI plays a critical role in the regulation of myofilament activation and LDA via three contiguous regions within its C-terminus: the inhibitory region (residues 130–150), the switch region (residues 151–167), and the mobile domain (residues 168–210). The inhibitory region of cTnI is mainly responsible for inhibiting muscle contraction via binding to actin during diastole [41, 42]. The switch region of cTnI binds to the hydrophobic cleft of Ca^{2+} bound cTnC initiating a series of allosteric conformational changes in the thin filament as mentioned above [9, 10, 13]. The cTnI-MD has been shown to stabilize the actin-cTnI interaction at low levels of Ca^{2+} concentration [43]. The cTnI-MD is a highly conserved region which is required for the full inhibition of the actomyosin MgATPase activity [43, 44]. Mutations within the MD have been associated with hypertrophic cardiomyopathy [45–48], restrictive cardiomyopathy [47–50], and dilated cardiomyopathy [47, 48, 51]. The functional importance of cTnI-MD is believed to be associated with the unique structural properties of the region. The cTnI-MD is intrinsically

Author Manuscript Author Manuscript Author Manuscript Author Manuscript

disordered, and undergoes a disordered-ordered structural transition while interacting with actin, allowing the cTnI-MD to perform its fly-casting activity to rapidly initiate the relaxation [16, 52–54]. The C-terminal end segment of cTnI-MD (residues 193–210) has been shown to interact with tropomyosin [55] and cTnC [56] in a Ca^{2+}-sensitive manner and to help restrict tropomyosin position at diastole. The C-terminal deletion of cTnI, residues 193–210, is found to be associated with myocardial stunning [57, 58]. Our knowledge from these studies strongly suggest that cTnI-MD plays an important role in maintaining healthy heart function via its dynamic interaction with the actin filament. However, it is unclear how the dynamic interactions between the cTnI-MD and the actin filament influences cross-bridge cycling and force production as Ca^{2+} concentration and SL change, and how the MD affects the balance between thin filament vs. thick filament regulation of LDA.

In this study, two C-terminus truncations of cTnI were chosen to investigate the functional significance of the cTnI-MD in myocardial tension development and the kinetics of cross-bridge cycling at different Ca^{2+} concentrations and SLs. The first, cTnI(1–167), effectively removes the entire MD; and the second, cTnI(1–193), removes only the last 17 amino acids of cTnI. These truncations were exchanged with endogenous cTnI in skinned rat papillary muscle fibers. Our results show that the entire MD truncation diminished the SL-induced increase in Ca^{2+}-sensitivity of myocardial contraction, but did not affect the SL-induced increase in maximal developed tension, suggesting an uncoupling between thin filament- and thick filament-based regulation of LDA. This potential uncoupling due to the MD truncation highlights the role of this region in balancing the interplay between thin and thick filament mechanisms that, in combination, underlie LDA of cardiac contractility.

2. Materials and methods

2.1. Animal models

The handling of all experimental animals was approved by the Institutional Animal Care and Use Committee at Washington State University and complied with the *Guide for the Use and Care of Laboratory Animals* published by the National Institutes of Health. Our muscle preparation study also followed the established guidelines of and was approved by the Washington State University Institutional Animal Care and Use Committee. Rats were anesthetized by isoflurane inhalation (3% volume in 95% O2–5% CO2 flowing at 2 l/min), following which hearts were immediately excised and placed in dissecting solution on ice.

2.2. Preparation of proteins

Wild-type recombinant cTnC, cTnI and cTnT were overexpressed in Escherichia coli strain BL21(DE3) cells (Invitrogen) and purified as described previously [8, 9, 12]. The C-terminus truncations of cTnI, cTnI(1–167) and cTnI(1–193), were constructed by site-directed mutagenesis from rat cTnI cDNA clones and then sub-cloned into the pET-3d vector according to the manufacturer's protocols (GenScript). The truncated cTnI clones were then transformed into BL21(DE3) cells and expressed under isopropyl b-D-1-thiogalactopyranoside induction. The expressed proteins were purified as previously described for rat cTnI(WT) [8, 9, 12].

Author Manuscript Author Manuscript Author Manuscript Author Manuscript

2.3. Solutions for skinned myocardial strips

Muscle mechanics solution concentrations were formulated by solving equations describing ionic equilibria according to Godt and Lindley [59], and all concentrations are listed in mM unless otherwise noted. Dissecting solution: 50 N,N-Bis(2-hydroxyethyl)-2-aminoethanesulfonic acid (BES), 30.83 K propionate, 10 sodium azide (NaN_3), 20 ethylene glycol-bis(β-aminoethyl ether)-N,N,N',N'-tetraacetic acid (EGTA), 6.29 $MgCl_2$, 6.09 ATP, 1 Dithiothreitol (DTT), 20 2,3-Butanedione monoxime (BDM), 50 μM Leupeptin, 275 μM Pefabloc, and 1 μM E-64. Skinning solution: dissecting solution with 1% Triton-X100 wt/vol and 50% glycerol wt/vol. Storage solution: dissecting solution and 50% glycerol wt/vol. Relaxing solution: pCa 8.0 ($pCa = -\log_{10}[Ca^{2+}]$), 5 EGTA, 5 MgATP, 1 Mg^{2+}, 0.3 P_i, 35 phosphocreatine, 300 U/mL creatine kinase, 200 ionic strength, pH 7.0. Activating solution: same as relaxing with pCa 4.8. Rigor solution: same as activating solution without MgATP.

2.4. Incorporation of cTnI(1–167)/cTnI(1–193) into detergent skinned myocardial fibers

Cardiac troponin complex containing wild-type cTnC, cTnI(1–167) or cTnI(1–193) and wild-type cTnT was reconstituted at a molar ratio of 1:1:1 cTnC:cTnI:cTnT using a protocol published previously [40, 60]. Endogenous troponin in the detergent skinned rat papillary muscle fibers were exchanged by overnight incubation of fibers in exchange solution containing 25μM of reconstituted cTn complex followed by another overnight incubation of fibers in exchange solution containing 10μM of only cTnC. The same exchange procedure was followed using wild-type cTnI that served as our control fibers. The exchange solution contained (in mM): 50 BES, 30.83 K-propionate, 10 NaN_3, 20 EGTA, 6.29 $MgCl_2$, 6.09 Na_2ATP, 20 BDM,1 DTT, 0.005 bestatin, 0.002 E-64, 0.01 leupeptin, and 0.001 pepstatin.

2.5. Skinned myocardial strips

Left ventricular papillary muscles were dissected from three hearts and trimmed down to thin strips (~180 μm in diameter and 700 μm long). Strips were skinned overnight at 4 °C and stored at −20 °C for up to one week. Aluminum T-clips were attached to the end of each strip and strips were mounted between a piezoelectric motor (P841.40, Physik Instrumente, Auburn, MA) and a strain gauge (AE801, Kronex, Walnut Creek, CA), lowered into a 30 μL droplet of relaxing solution maintained at 17 °C, and stretched to 1.9 or 2.2μm SL measured by digital Fourier Transform (IonOptix Corp, Milton, MA). These strips were calcium activated from pCa 8.0 to pCa 4.8 and then [MgATP] was titrated towards rigor ([MgATP] < 0.05 mM).

2.6. Western blotting analysis of reconstitution levels of modified cTnI in cardiac muscle

To assess the efficiency of the protein exchange using our protocol, the reconstituted muscle fibers with cTnI truncations were incubated in 10 μL of a protein extraction buffer per 1 muscle fiber on ice for 1 h. Skinned muscle fibers that had not undergone exchange were similarly incubated to create a negative control. The protein extraction buffer contained 2.5% SDS, 10% glycerol, 50 mM Tris-base (pH 6.8 at 4 °C), 1 mM DTT, 1 mM phenylmethylsulfonyl fluoride, 4mM benzamidine HCl, 5 μM bestatin, 2 μM E-64, 10 μM leupeptin and 1 μM pepstatin. The incubation was followed by a 20-minute sonication of

Author Manuscript Author Manuscript Author Manuscript Author Manuscript

samples in a water bath at 4°C and centrifugation at 10k rpm. Equal amounts of supernatants fractions were loaded to 4–20% SDS-PAGE gels for Western blotting analysis following the protocol established previously [40, 61, 62]. Loading amounts were standardized by estimating the total protein concentration using a Protein Assay Kit (Biorad #5000121). The incorporation of cTnI-MD truncations was evaluated using a primary antibody against cTnI (Abcam #19615) followed by horseradish peroxidase conjugated anti-mouse antibody (GE healthcare NXA931).

2.7. Dynamic mechanical analysis

Stochastic length perturbations were applied for a period of 60 s using an amplitude distribution with a standard deviation of 0.05% muscle length over the frequency range 0.5–250 Hz as previously described [63, 64]. Elastic and viscous moduli, E(ω) and V(ω), were measured as a function of angular frequency (ω) from the in-phase and out-of-phase portions of the tension response to the stochastic length perturbation. The complex modulus, Y(ω), was defined as E(ω) + iV(ω), where i = √−1.

Estimates of six model parameters (A, k, B, 2πb, C, 2πc) were provided by fitting Eq. (1) to the entire frequency range of moduli values.

$$\mathrm{Y}(\omega)=\mathrm{A}(\mathrm{i}\omega)^{k} - B\left(\frac{i\omega}{2\pi b+i\omega}\right)+C\left(\frac{i\omega}{2\pi c+i\omega}\right) \quad (1)$$

The A-, k-, B-, and C-terms in Eq. (1) related to viscoelasticity and cross-bridge binding are discussed in detail in the online data supplement. Herein, we focus on the kinetic parameters of cross-bridge cycling (i.e. cross-bridge attachment and detachment rates).

Rate parameters 2πb and 2πc reflect cross-bridge kinetics that are sensitive to biochemical perturbations affecting enzymatic activity, such as [MgATP], [MgADP], or [P_i] [65]. Molecular processes contributing to cross-bridge recruitment or force generation correspond to the cross-bridge attachment rate (2πb). Similarly, processes contributing to cross-bridge detachment or force decay correspond to the cross-bridge detachment rate (2πc). The cross-bridge detachment rate can be described by Eq. (2):

$$2\pi\mathrm{c}=\frac{k_{-\mathrm{ADP}}[\mathrm{MgATP}]}{\frac{k_{-\mathrm{ADP}}}{k_{+\mathrm{ATP}}}+[\mathrm{MgATP}]} \quad (2)$$

As explained by Tyska and Warshaw [66] and implemented by Tanner et al. [67, 68], fitting the 2πc-[MgATP] relationship to Eq. (2) allow us to calculate 1) cross-bridge MgADP release rate (k_{-ADP}) and the asymptotic, maximal myosin detachment rate in s^{-1} at saturating [MgATP]; and 2) cross-bridge MgAP binding rate in M^{-1} s^{-1} (k_{+ATP}).

Author Manuscript Author Manuscript Author Manuscript Author Manuscript

2.8. Statistical analysis

All values are means ± SE. Constrained nonlinear least squares fitting of Eqs. (1) and (2) to the data was performed using sequential quadratic programming methods in Matlab (v 7.9.0; The Mathworks, Natick, MA). Three-way ANOVA followed by Tukey post-test was used to examine the influence of SL, truncation, pCa, and the interaction effect between these three independent variables on the developed tension-pCa relationship. Two-way ANOVA followed by Tukey post-test was used to examine the influence of SL, truncation and their interaction effect on all the fit parameters to a 3-parameter Hill equation for normalized tension-pCa relationship. Two-way ANOVA analysis was performed to examine the difference between two SLs on the MgATP dependent parameter estimates from modulus data fit to Eq. (1) for fibers containing cTnI(WT). To compare fibers containing cTnI(1–167) to cTnI(1–193) and to compare them to cTnI(WT) fibers, three-way ANOVA was performed. Three-way ANOVA followed by Tukey post-test was used to examine the influence of SL, truncation, [MgATP], and the interaction effect between these three independent variables on the MgATP dependent parameter estimates from modulus data fit to Eq. (1). All statistical analysis was done using GraphPad Prism 7.01. Statistical significance is reported at $P < 0.05$.

3. Results

3.1. Western blot analysis of the reconstituted cardiac muscle fibers

To estimate the relative amount of cTnI (1–167) and cTnI(1–193) that was incorporated into the samples, equal quantities of digested muscle fiber samples were separated on SDS-PAGE gels followed by western blotting analysis (Fig. 1). The differences in migration speed between the cTnI(1–167)/cTnI(1–193) and the endogenous cTnI showed 64% ± 5 relative incorporation of both cTnI(1–167) and cTnI(1–193) in skinned cardiac muscle fibers.

3.2. Isometric tension-pCa relationships

Isometric tension developed in a sigmoidal manner as a function of pCa for fibers when either cTnI(WT), cTnI(1–167), or cTnI(1–193) was exchanged for endogenous cTnI (Fig. 2). These tension-pCa relationships were fit to a 3-parameter Hill equation, with the estimated parameters shown in Fig. 3 and listed in Table 1. As SL increased from 1.9 to 2.2μm, the maximal developed tension increased for fibers containing either of the truncated cTnIs, as well as the cTnI(WT) ($P < 0.001$ for the SL effect and pCa × SL interaction; Fig. 2). Different cTnI-MD truncations influenced the maximal developed tension to various extents as SL varied ($P < 0.001$ for truncation effect, truncation × SL interaction, and pCa × truncation × SL interaction; Fig. 2B & C). Under maximally activated conditions, cTnI(1–167) increased the developed tension by 2.2-fold at short SL and 1.6-fold at long SL, compared to cTnI(WT) ($P < 0.001$ for truncation and truncation × SL; Fig. 3B). In contrast, the cTnI(1–193) truncation showed no significant effects on the maximal developed tension at both SLs, based on a two-way ANOVA (Fig. 3A and 3B). However, there was a significant interaction between the cTnI(1–193) truncation and SL for maximal developed tension ($P < 0.001$; Fig. 3A & B), which shows that the cTnI(1–193) truncation affects tension development differently at short vs. long SL. Compared to cTnI(WT), the cTnI(1–

Author Manuscript Author Manuscript Author Manuscript Author Manuscript

193) truncation resulted in a slight increase in maximal developed tension at short SL and a 14.3% decrease in maximal developed tension at long SL (Table 1), but these modest tension differences were not statistically significantly.

Another novel observation from the isometric tension-pCa relationships (Fig. 2) is the truncation effects on SL-induced changes on the Ca^{2+}-sensitivity and cooperativity of contraction. Fibers containing cTnI(WT) showed a SL-dependent increase in Ca^{2+}-sensitivity (ΔpCa_{50}=0.08) that accompanied greater cooperativity as SL increased ($P < 0.001$ for the SL effect; Fig. 3C – F and Table 1). The cTnI(1–167) fibers showed no significant increases in Ca^{2+}-sensitivity and cooperativity with increase in SL (Fig. 3C – F), suggesting SL-induced changes in Ca^{2+}-sensitivity and cooperativity of myocardial fibers are diminished by truncating the entire cTnI-MD. Similar to cTnI(WT), cTnI(1–193) fibers showed SL-dependent increases in Ca^{2+}-sensitivity (ΔpCa_{50}=0.09) and cooperativity as SL increased from 1.9 to 2.2μm.

Analysis of the isometric tension-pCa relationships also provides information regarding the role of truncations on thin filament-based regulation of myocardial tension development. Compared to cTnI(WT), the cTnI(1–167) truncation was more sensitive to [Ca^{2+}] at both SLs, which also accompanied increased cooperativity (Table 1). The cTnI(1–193) truncation also increased Ca^{2+}-sensitivity of the force-pCa relationship at both SLs, compared to cTnI(WT). However, the cooperativity coefficient (nH) was similar for cTnI(1–193) and cTnI(WT) at either SL (Fig. 3). Despite the shift in the Ca^{2+}-sensitivity and maximal tension for cTnI(1–93) compared to cTnI(WT), the SL-induced increase in Ca^{2+}-sensitivity and maximal tension behaves in a similar fashion—suggesting the thin filament aspects are preserved for cTnI(1–193) in a manner that is consistent with the cTnI(WT) results.

3.3. The effects of sarcomere length on the kinetics of cross-bridge cycling for myocardial fibers containing cTnI(WT) and cTnI-MD truncations

Moduli values obtained from our stochastic length perturbations (described in online data supplement) were fit to Eq. (1) to extract model parameters related to myocardial viscoelasticity, cross-bridge binding, and cross-bridge kinetics under maximally activated (pCa 4.8) conditions as [MgATP] varied from 5 to 0.05 mM. Model parameters related to cross-bridge attachment rate ($2\pi b$) and detachment rate ($2\pi c$) are plotted against [MgATP] in Fig. 4, with the resulting *P*-values listed within each panel for significant effects of [MgATP], SL, or truncation as well as any significant interaction effects between each of these variables.

In this section, we will discuss model parameters related to the kinetics of cross-bridge cycling, with a focus on the effects of SL within fibers containing cTnI(WT) or cTnI-MD truncations. As [MgATP] decreased, the cross-bridge attachment rate ($2\pi b$) and cross-bridge detachment rate ($2\pi c$) slowed at both short and long SLs for fibers containing cTnI(WT) and both cTnI-MD truncations (Fig. 4). There was not a significant effect of SL on the rate of cross-bridge attachment for cTnI(WT) fibers (Fig. 4A). However, cTnI(1–167) and cTnI(1–193) both showed a faster cross-bridge attachment rate as SL increased from 1.9 to 2.2μm ($P < 0.001$ for SL and [MgATP]; Fig. 4B & C). Fibers containing cTnI(WT) showed a significantly slower cross-bridge detachment rate as SL increased from 1.9 to 2.2μm (*P*

Author Manuscript Author Manuscript Author Manuscript Author Manuscript

<0.001 for SL and [MgATP] × SL interaction effect; Fig. 4D). Cross-bridge detachment rate was more sensitive to [MgATP] at 1.9 vs. 2.2μm SL for cTnI(WT) fibers (interaction effect between [MgATP] × SL), evident by a greater decrease in the value of 2πc over the entire range of [MgATP] at 1.9μm SL. This finding may follow from a greater dynamic range for cross-bridge detachment at shorter SL that results in a steeper decrease in cross-bridge detachment rate (Fig. 4D). Fibers containing cTnI(1–167) showed a modest SL effect on cross-bridge detachment rate, with 2πc-MgATP response shifting toward slower detachment rate values as SL increased from 1.9 to 2.2μm (P <0.001 for [MgATP] × SL interaction effect; Fig. 4E). The cTnI(1–193) fibers showed a slightly slower cross-bridge detachment rate at longer SL (P <0.001 for SL and [MgATP] × SL interaction effect; Fig. 4F).

To link the cross-bridge detachment rate with the cross-bridge rate of MgADP release (k_{-ADP}), and the cross-bridge rate of MgATP binding (k_{+ATP}), the 2πc-MgATP relationships were fit to Eq. 2 [63, 67–69] (Fig. 4D – F). This analysis showed that increasing SL slowed MgADP release for cTnI(WT) and both cTnI-MD truncations, but MgATP binding rates were not statistically different between short and long SLs among all constructs (Table 2).

3.4. The effects of cTnI-MD truncations on the kinetics of cross-bridge cycling at both short and long sarcomere lengths

We will now discuss the effects of cTnI-MD truncations on cross-bridge cycling kinetics among all constructs. Compared to cTnI(WT), both cTnI(1–167) and cTnI(1–193) fibers led to faster cross-bridge attachment rates at both SLs (Fig. 4B & C). However, the cTnI(1–167) truncation significantly slowed the rate of cross-bridge detachment at short SL, compared to cTnI(WT) fibers (P <0.001 for truncation and truncation × SL effect; Fig. 4E). In contrast, the cTnI(1–193) truncation sped cross-bridge detachment rate at long SL, compared to cTnI(WT) (significant truncation, truncation × SL, and [MgATP] × truncation × SL interaction effects; Fig. 4F). These SL-dependent differences between the rates of cross-bridge attachment and detachment for cTnI(1–167) and cTnI(1–193) in comparison to cTnI(WT), may imply different roles for the different regions of cTnI-MD in regulating thin vs. thick filament contributions to LDA of contraction in cardiac muscle.

4. Discussion

The objective of this study was to better understand the regulatory role of cTnI-MD in Ca^{2+}- and SL-induced myocardial tension development and cross-bridge cycling. Our results suggest that the MD is critical to the regulatory role of cTnI in modulating myocardial Length dependent activation, particularly the thin filament-based regulations. Each region within the cTnI-MD plays unique role in Ca^{2+}-activated and SL-induced tension development of myocardium as we will discuss in this section. To facilitate the comparison between cTnI-MD truncations and cTnI(WT), we prepared a table to qualitatively summarize the functional effects of each cTnI-MD truncations on myocardial tension development and kinetics of cross-bridge cycling compared to cTnI(WT) (Supplemental Table 1).

Tension production and Ca^{2+}-sensitivity of contraction increase as SL increases; these key characteristics of physiological cardiac muscle function are known as length-dependent

Author Manuscript Author Manuscript Author Manuscript Author Manuscript

activation (LDA). The mechanisms underlying LDA are complicated, but recent studies suggest it involves multiple regulatory components of the myofilaments [26–39]. This dual-filament regulation includes: i) thin filament-based regulation that is reflected by SL-induced increases in Ca^{2+} sensitivity and/or cooperativity of the force-pCa relationship, ii) thick filament-based regulation that is reflected by SL-induced increases in cross-bridge binding, cycling behavior, and/or tension development, and iii) the coupled interplay between these regulatory pathways.

The results of our SL-dependent functional study for myocardial fibers containing cTnI(WT) (Fig. 2A and Table1), are consistent with previous studies [70–74]. Similar SL-induced behavior, increased maximal tension, Ca^{2+}-sensitivity, and cooperativity of contraction, was observed when cTnI(WT) was replaced by cTnI(1–193) (Fig. 2C and Fig. 3), suggesting that both thin filament- and thick filament-based regulatory mechanisms of LDA were preserved with the cTnI(1–193) truncation. This result implies that the C-terminus truncation of the MD, cTnI(1–193), does not perturb the regulatory role of cTnI-MD in SL-induced function of myocardium, despite the shift in the absolute values of pCa_{50} at both short and long SLs. In contrast, truncating the entire MD via cTnI(1–167) led to greater force and greater cross-bridge binding at longer SL (consistent with greater values of B and C as SL increased from 1.9 to 2.2μm; Supplemental Fig. 2H & K), thereby suggesting that cTnI(1–167) preserved thick filament-based regulation of LDA. However, cTnI(1–167) eliminated the SL-induced increases in Ca^{2+}-sensitivity and cooperativity (Fig. 2B and Table 1), suggesting that cTnI(1–167) perturbed thin filament-based regulatory mechanisms of LDA and the interplay between thin filament- and thick filament-based mechanisms of LDA. These observations are significant because they show how the cTnI-MD contributes to the LDA by directly or indirectly sensing the effects of SL changes on the thin filament.

The cTnI-MD may help balance the interplay between different regulatory components of SL-dependent myocardial function. Thus, truncating the cTnI-MD perturbs this balance and uncouples the SL-induced effects on tension development (i.e. thick filament regulation mechanisms) from the thin filament-based regulation mechanisms. This speculation is consistent with the recent study by Zhang et al. (2017) which shows distinctive effects of SL on thin and thick filaments [27]. Specifically, they found that the SL-induced structural changes in Tn are distinct from those caused by Ca^{2+} activation or strongly bound cross-bridges, and SL-induced structural changes in myosin is responsible for the increased maximal force. Our study suggests that the region between residues 167 and 193 of cTnI-MD is important to sense and/or transmit the effects of the SL change to the regulatory domain of cTnC, and this region may play an important role in mediating the level of thin filament activation that is modulated with SL changes. It should be noted that our results do not exclude the possibility that the removing the entire cTnI-MD saturates the Ca^{2+}-sensitivity and cooperativity of contraction, therefore, further increasing SL would not further enhance these effects. Additional structure-function studies are needed in the future to illustrate the detailed regulatory role of different regions of the MD in LDA.

Truncating the MD to various extents exhibited different effects on Ca^{2+}-activated regulation of tension development and cross-bridge kinetics. The increased maximum tension, Ca^{2+}-sensitivity and cooperativity of cTnI(1–167) compared to cTnI(WT) fibers may be due to a

Author Manuscript Author Manuscript Author Manuscript Author Manuscript

partial loss of the inhibitory function after deletion of the cTnI-MD, which contains the second actin-binding region of the C-terminus of cTnI (residues 170–181). This weakens the interaction between cTnI and actin to promote actomyosin binding, which could then further sensitize the myofilaments to Ca^{2+} [75]. We also speculate that poor inhibition by the truncated cTnI-MD may allow azimuthal Tm movement in the regulatory unit to promote actomyosin binding, which could also enhance cooperative feedback on thin filament regulatory units [76–80]. The cTnI(1–167) truncation could also impair myofibrillar relaxation due to the loss of MD sampling arm, leading to the enhanced Ca^{2+}-sensitivity of contraction and cooperative activation of thin filament during the contraction cycle.

Enhanced myofilament Ca^{2+}-sensitivity at both short and long SLs for cTnI(1–193) fibers suggests a partial loss of inhibitory function after deletion of the last 17 amino acids of cTnI. Metskas et al. [82] have suggested in the closed state of Tm, cTnI-MD around residues 193–210 stays bound to actin and retains a conformation similar to the blocked state while it is dynamic and unbound between residues 161–192 [82]. In this regard, a previous study by Zhang et al. suggested that the end segment of the C-terminus of cTnI (residues 193–210) binds to Tm [55] and TnC [56] in a Ca^{2+} sensitive manner, and helps to restrict Tm movement in the relaxed condition [55]. These studies suggest that losing this segment could potentially affect the position and/or flexibility of Tm in the relaxed state promoting actomyosin binding, which agrees with our findings as well.

The increased Ca^{2+}-sensitivity of force development for cTnI(1–193) fibers contrasts with our observation of no significant difference in maximal developed tension at short SL and a 14.3% decrease at long SL, yet not statistically significant, based on a two-way ANOVA. However, excluding the SL variant and performing one-way ANOVA at long SL shows a significant reduction in maximal developed tension, consistent with other studies [81].

Based on the two-state cross-bridge model, the amount of tension development depends on the ratio of cross-bridge attachment rate ($2\pi b$) to the sum of cross-bridge attachment and detachment rates ($2\pi b+2\pi c$). Our kinetic results at 1.9 μm SL show a faster attachment rate for cTnI(1–193) compared to cTnI(WT), with no significant effect on detachment rate. Considering the range of $2\pi b$ and $2\pi c$, a small increase in $2\pi b$ would not dramatically change the ratio of $2\pi b/(2\pi b+2\pi c)$ for cTnI(1–193) at short SL. At a SL of 2.2 μm, both attachment and detachment rates were significantly faster in fibers containing cTnI(1–193), with a greater increase in $2\pi c$, which together would decrease the ratio of $2\pi b/(2\pi b+2\pi c)$ at long SL. These kinetic effects are consistent with cross-bridge cycling measurement by Gao et al. (2006) who observed a faster rate of force redevelopment (k_{tr}) in stunned muscle [83].

The cTnI(1–193) truncation showed no significant effect on the cooperativity of myocardial contraction with the 64±5% exchange of the endogenous cTnI with cTnI(1–193). Different from our results, Tachampa et al. [81] observed a 50% decrease in cooperativity of contraction upon both 70% and 50% exchange of endogenous cTnI with cTnI(1–193). Thus, we rule out the possibility of residual endogenous cTnI masking the effects of the partially exchanged truncated cTnI in our study, since the similar exchange ratio of cTnI(1–167) resulted in a significant increase of the cooperativity of contraction in our study. The

Author Manuscript Author Manuscript Author Manuscript Author Manuscript

differences among studies could be attributed to differences in buffer formulation, sample preparation, applied measuring techniques, and equipment.

Our results for cTnI(1–167) showed a greater viscoelastic mechanical response of the passive elements compared to cTnI(WT) fibers, evident by the significant increase in parameter *A* and decrease in parameter *k* at both SLs (Supplemental Fig. 2B&E, in the online data supplement). A study by Fusi et al. showed a direct control of thick filament activation by the thick filament stress which occurs independent of intracellular Ca^{2+} concentration [31]. Considering this study, the increase in passive elements with cTnI-MD truncation could possibly affect the orientation and structure of myosin motors that increases the number of myosin heads available for cross-bridge binding. This effect of cTnI-MD truncation on the thick filament works in synergy with the increase in the number of available myosin-binding sites on actin induced by Tm movement, to increase the cross-bridge attachment rate and the force of contraction observed for cTnI(1–167) fibers.

The cTnI(1–193) showed faster cross-bridge attachment rates at both SLs and faster cross-bridge detachment rates at long SL compared to cTnI(WT). Consistent with our results, previous studies using skinned rat cardiac trabeculae containing cTnI(1–193) at 2.2 μm SL showed increased tension cost and enhanced rate of force redevelopment [81]. Thus, the cTnI(1–193) truncation may shift the average position of Tm to a new equilibrium position that more closely resembles the myosin-induced open-state [58, 85].

5. Conclusions

This study provides valuable information about the role of the C-terminus of cTnI in contractile regulation and LDA. The region between residues 167 and 193 of cTnI plays a critical role in cardiac contractility by mediating the level of thin filament activation, which is also modulated by SL changes. Our results for cTnI(1–167) suggest that the cTnI-MD plays a role in LDA by sensing/transmitting the effects of SL to the core of the regulatory Tn-Tm complex, and that removing this region perturbs the balance between thin filament- and thick filament-based regulation of LDA. Furthermore, the cTnI-MD helps to maintain the equilibrium position of Tm at both relaxed and activated states, which can potentially modulate LDA through the feedback effects of strong cross-bridges on the thin filament.

Supplementary Material

Refer to Web version on PubMed Central for supplementary material.

Acknowledgments

We thank Peter Awinda for his help throughout data acquisition, Axel Fenwick for his help on the data analysis, and William Schlecht for helpful comments on the manuscript. This work is supported by National Institutes of Health Grants R01 HL80186 (WJD), R21 HL109693 (WJD), and by the M. J. Murdock Charitable Trust (WJD), and American Heart Association grants 17GRNT33460153 (WJD), 14BGIA20380385 (BCWT), 17SDG33370153 (BCWT).

Abbreviations

cTnC cardiac troponin C

Author Manuscript Author Manuscript Author Manuscript Author Manuscript

cTnI	cardiac troponin I
cTnT	cardiac troponin T
cTnI-MD	mobile domain of cardiac troponin I
cTnI(WT)	wild-type cTnI
SL	sarcomere length
LDA	length dependent activation
BES	N,N-Bis(2-hydroxyethyl)-2-aminoethanesulfonic acid
EGTA	ethylene glycol-bis(β-aminoethyl ether)-N,N,N',N'-tetraacetic acid
DTT	Dithiothreitol
BDM	2,3-Butanedione monoxime

References

1. Gordon AM, Homsher E, Regnier M. Regulation of contraction in striated muscle. Physiol Rev. 2000; 80(2):853–924. [PubMed: 10747208]
2. Leavis PC, Gergely J. Thin filament proteins and thin filament-linked regulation of vertebrate muscle contraction. CRC Crit Rev Biochem. 1984; 16(3):235–305. [PubMed: 6383715]
3. Zot AS, Potter JD. Structural aspects of troponin-tropomyosin regulation of skeletal muscle contraction. Annu. Rev. Biophys. Biophys. Chem. 1987; 16:535–559. [PubMed: 2954560]
4. Tobacman LS. Thin Filament-Mediated Regulation of Cardiac Contraction. Annual Review of Physiology. 1996; 58(1):447–481.
5. Parry DA, Squire JM. Structural role of tropomyosin in muscle regulation: analysis of the x-ray diffraction patterns from relaxed and contracting muscles. J. Mol. Biol. 1973; 75(1):33–55. [PubMed: 4713300]
6. Huxley HE. Structural changes in the actin-and myosin-containing filaments during contraction. Cold Spring Harbor Symp. Qant. Biol. 1972; 37:361–376.
7. Li MX, Spyracopoulos L, Sykes BD. Binding of cardiac troponin-I147–163 induces a structural opening in human cardiac troponin-C. Biochemistry. 1999; 38(26):8289–98. [PubMed: 10387074]
8. Dong WJ, et al. Conformation of the regulatory domain of cardiac muscle troponin C in its complex with cardiac troponin I. J Biol Chem. 1999; 274(44):31382–90. [PubMed: 10531339]
9. Dong WJ, et al. Ca^{2+} induces an extended conformation of the inhibitory region of troponin I in cardiac muscle troponin. J. Mol. Biol. 2001; 314(1):51–61. [PubMed: 11724531]
10. Kobayashi T, et al. Inhibitory region of troponin I: Ca(2+)-dependent structural and environmental changes in the troponin-tropomyosin complex and in reconstituted thin filaments. Biochemistry. 2000; 39(1):86–91. [PubMed: 10625482]
11. Wei B, Jin JP. Troponin T isoforms and posttranscriptional modifications: Evolution, regulation and function. Arch. Biochem. Biophys. 2011; 505(2):144–154. [PubMed: 20965144]
12. Robinson JM, et al. Switching of troponin I: Ca(2+) and myosin-induced activation of heart muscle. J Mol Biol. 2004; 340(2):295–305. [PubMed: 15201053]
13. Dong WJ, et al. Ca2+-induced conformational transition in the inhibitory and regulatory regions of cardiac troponin I. J Biol Chem. 2003; 278(10):8686–92. [PubMed: 12511564]
14. Xing J, et al. Structural studies of interactions between cardiac troponin I and actin in regulated thin filament using Forster resonance energy transfer. Biochemistry. 2008; 47(50):13383–93. [PubMed: 19053249]

Author Manuscript Author Manuscript Author Manuscript Author Manuscript

15. Xing J, et al. Forster resonance energy transfer structural kinetic studies of cardiac thin filament deactivation. J Biol Chem. 2009; 284(24):16432–41. [PubMed: 19369252]
16. Zhou Z, et al. Structural dynamics of C-domain of cardiac troponin I protein in reconstituted thin filament. J Biol Chem. 2012; 287(10):7661–74. [PubMed: 22207765]
17. Brenner B, et al. Thin filament activation probed by fluorescence of N-((2-(iodoacetoxy)ethyl)-N-methyl)amino-7-nitrobenz-2-oxa-1,3-diazole-labeled troponin I i ncorporated into skinned fibers of rabbit psoas muscle. Biophys J. 1999; 77(5):2677–91. [PubMed: 10545368]
18. Lehman W, Craig R, Vibert P. Ca^{2+}-induced tropomyosin movement in Limulus thin filaments revealed by three-dimensional reconstruction. Nature. 1994; 368(6466):65–67. [PubMed: 8107884]
19. Haselgrove JC. X-ray evidence for a conformational change in the actin-containing filaments of vertebrate striated muscle. Cold Spring Harbor Symp. Qant. Biol. 1972; 37:341–352.
20. Holmes KC. The actomyosin interaction and its control by tropomyosin. Biophys. J. 1995; 68(4 Suppl):2S–5S. discussion 6S–7S.
21. Lehman W, et al. Tropomyosin and actin isoforms modulate the localization of tropomyosin strands on actin filaments. J. Mol. Biol. 2000; 302(3):593–606. [PubMed: 10986121]
22. Poole KJV, Evans G, Rosenbaum G, Lorenz M, Holmes KC. The effect of crossbridges on the calcium sensitivity of the structural change of the regulated thin filament. Biophys. J. 1995; 68:A365.
23. Cooke R. Actomyosin interaction in striated muscle. Physiol Rev. 1997; 77(3):671–97. [PubMed: 9234962]
24. McDonald KS, Moss RL. Osmotic compression of single cardiac myocytes eliminates the reduction in Ca2+ sensitivity of tension at short sarcomere length. Circ Res. 1995; 77(1):199–205. [PubMed: 7788878]
25. Fuchs F, Wang Y-P. Sarcomere Length Versus Interfilament Spacing as Determinants of Cardiac Myofilament Ca2+Sensitivity and Ca2+Binding. J. Mol. Cell. Cardiol. 1996; 28(7):1375–1383. [PubMed: 8841926]
26. Irving TC, et al. Myofilament lattice spacing as a function of sarcomere length in isolated rat myocardium. Am J Physiol Heart Circ Physiol. 2000; 279(5):H2568–73. [PubMed: 11045995]
27. Zhang X, et al. Distinct contributions of the thin and thick filaments to length-dependent activation in heart muscle. eLife. 2017; 6:e24081. [PubMed: 28229860]
28. Reconditi M, et al. Sarcomere-length dependence of myosin filament structure in skeletal muscle fibres of the frog. J Physiol. 2014; 592(5):1119–37. [PubMed: 24344169]
29. Farman GP, et al. Myosin head orientation: a structural determinant for the Frank-Starling relationship. Am. J. Physiol. - Heart C. 2011; 300(6):H2155–H2160.
30. Farman GP, et al. Impact of osmotic compression on sarcomere structure and myofilament calcium sensitivity of isolated rat myocardium. Am. J. Physiol. - Heart C. 2006; 291(4):H1847–H1855.
31. Fusi L, et al. Thick filament mechano-sensing is a calcium-independent regulatory mechanism in skeletal muscle. Nature Communications. 2016; 7:13281.
32. Irving T, et al. Thick-Filament Strain and Interfilament Spacing in Passive Muscle: Effect of Titin-Based Passive Tension. Biophysical Journal. 2011; 100(6):1499–1508. [PubMed: 21402032]
33. Fukuda N, et al. Titin-based modulation of active tension and interfilament lattice spacing in skinned rat cardiac muscle. Pflugers Arch. 2005; 449(5):449–57. [PubMed: 15688246]
34. Cazorla O, et al. Titin-based modulation of calcium sensitivity of active tension in mouse skinned cardiac myocytes. Circ. Res. 2001; 88(10):1028–35. [PubMed: 11375272]
35. Methawasin M, et al. Experimentally increasing titin compliance in a novel mouse model attenuates the Frank-Starling mechanism but has a beneficial effect on diastole. Circulation. 2014; 129(19):1924–36. [PubMed: 24599837]
36. Fukuda N, et al. Length dependence of tension generation in rat skinned cardiac muscle: role of titin in the Frank-Starling mechanism of the heart. Circulation. 2001; 104(14):1639–45. [PubMed: 11581142]

Author Manuscript Author Manuscript Author Manuscript Author Manuscript

37. Fukuda N, et al. Sarcomere length-dependent Ca2+ activation in skinned rabbit psoas muscle fibers: coordinated regulation of thin filament cooperative activation and passive force. J Physiol Sci. 2011; 61(6):515–23. [PubMed: 21901640]
38. Hannon JD, Martyn DA, Gordon AM. Effects of cycling and rigor crossbridges on the conformation of cardiac troponin C. Circ. Res. 1992; 71(4):984–991. [PubMed: 1516169]
39. Moss RL, Razumova M, Fitzsimons DP. Myosin crossbridge activation of cardiac thin filaments: implications for myocardial function in health and disease. Circ Res. 2004; 94(10):1290–300. [PubMed: 15166116]
40. Li KL, et al. In situ time-resolved FRET reveals effects of sarcomere length on cardiac thin-filament activation. Biophys J. 2014; 107(3):682–93. [PubMed: 25099807]
41. Nozaki S, et al. SYNTHETIC STUDIES ON TROPONIN I ACTIVE SITE. PREPARATION OF A PENTADECAPEPTIDE WITH INHIBITORY ACTIVITY TOWARD ACTOMYOSIN ADENOSINE TRIPHOSPHATASE. Chemistry Letters. 1980; 9(3):345–348.
42. Talbot JA, Hodges RS. Synthetic studies on the inhibitory region of rabbit skeletal troponin I. Relationship of amino acid sequence to biological activity. J. Biol. Chem. 1981; 256(6):2798–2802. [PubMed: 6451620]
43. Murakami K, et al. Structural basis for Ca2+-regulated muscle relaxation at interaction sites of troponin with actin and tropomyosin. J Mol Biol. 2005; 352(1):178–201. [PubMed: 16061251]
44. Rarick HM, et al. The C terminus of cardiac troponin I is essential for full inhibitory activity and Ca^{2+} sensitivity of rat myofibrils. J. Biol. Chem. 1997; 272(43):26887–26892. [PubMed: 9341121]
45. Takahashi-Yanaga F, et al. Functional consequences of the mutations in human cardiac troponin I gene found in familial hypertrophic cardiomyopathy. J Mol Cell Cardiol. 2001; 33(12):2095–107. [PubMed: 11735257]
46. Kimura A, et al. Mutations in the cardiac troponin I gene associated with hypertrophic cardiomyopathy. Nat Genet. 1997; 16(4):379–82. [PubMed: 9241277]
47. Lu Q-W, Wu X-Y, Morimoto S. Inherited cardiomyopathies caused by troponin mutations. Journal of Geriatric Cardiology : JGC. 2013; 10(1):91–101. [PubMed: 23610579]
48. Mogensen J, Hey T, Lambrecht S. A Systematic Review of Phenotypic Features Associated With Cardiac Troponin I Mutations in Hereditary Cardiomyopathies. Can J Cardiol. 2015; 31(11):1377–85. [PubMed: 26440512]
49. Mogensen J, et al. Idiopathic restrictive cardiomyopathy is part of the clinical expression of cardiac troponin I mutations. The Journal of Clinical Investigation. 111(2):209–216.
50. Yumoto F, et al. Drastic Ca2+ sensitization of myofilament associated with a small structural change in troponin I in inherited restrictive cardiomyopathy. Biochem Biophys Res Commun. 2005; 338(3):1519–26. [PubMed: 16288990]
51. Carballo S, et al. Identification and functional characterization of cardiac troponin I as a novel disease gene in autosomal dominant dilated cardiomyopathy. Circ Res. 2009; 105(4):375–82. [PubMed: 19590045]
52. Hoffman RMB, Blumenschein TMA, Sykes BD. An Interplay between Protein Disorder and Structure Confers the Ca2+ Regulation of Striated Muscle. Journal of Molecular Biology. 2006; 361(4):625–633. [PubMed: 16876196]
53. Blumenschein TM, et al. Dynamics of the C-terminal region of TnI in the troponin complex in solution. Biophys J. 2006; 90(7):2436–44. [PubMed: 16415057]
54. Jayasundar JJ, et al. Molecular dynamics simulations of the cardiac troponin complex performed with FRET distances as restraints. PLoS ONE. 2014; 9(2):e87135. [PubMed: 24558365]
55. Zhang Z, et al. Calcium-regulated conformational change in the C-terminal end segment of troponin I and its binding to tropomyosin. Febs j. 2011; 278(18):3348–59. [PubMed: 21777381]
56. Ferrieres G, et al. Systematic mapping of regions of human cardiac troponin I involved in binding to cardiac troponin C: N- and C-terminal low affinity contributing regions. FEBS Lett. 2000; 479(3):99–105. [PubMed: 10981715]
57. Narolska NA, et al. Impaired diastolic function after exchange of endogenous troponin I with C-terminal truncated troponin I in human cardiac muscle. Circ Res. 2006; 99(9):1012–20. [PubMed: 17023673]

Author Manuscript Author Manuscript Author Manuscript Author Manuscript

58. Galińska A, et al. The C-terminus of cardiac troponin I stabilizes the Ca(2+)-activated state of tropomyosin on actin filaments. Circulation research. 2010; 106(4):705–711. [PubMed: 20035081]
59. Godt RE, Lindley BD. Influence of temperature upon contractile activation and isometric force production in mechanically skinned muscle fibers of the frog. J Gen Physiol. 1982; 80(2):279–97. [PubMed: 6981684]
60. Li KL, et al. Sarcomere length dependent effects on the interaction between cTnC and cTnI in skinned papillary muscle strips. Arch Biochem Biophys. 2016; 601:69–79. [PubMed: 26944554]
61. Rieck DC, et al. Structural basis for the in situ Ca(2+) sensitization of cardiac troponin C by positive feedback from force-generating myosin cross-bridges. Arch Biochem Biophys. 2013; 537(2):198–209. [PubMed: 23896515]
62. Tsaturyan AK, et al. Strong Binding of Myosin Heads Stretches and Twists the Actin Helix. Biophysical Journal. 2005; 88(3):1902–1910. [PubMed: 15596509]
63. Tanner BC, Breithaupt JJ, Awinda PO. Myosin MgADP release rate decreases at longer sarcomere length to prolong myosin attachment time in skinned rat myocardium. Am J Physiol Heart Circ Physiol. 2015; 309(12):H2087–97. [PubMed: 26475586]
64. Tanner BC, et al. Measuring myosin cross-bridge attachment time in activated muscle fibers using stochastic vs. sinusoidal length perturbation analysis. J Appl Physiol (1985). 2011; 110(4):1101–8. [PubMed: 21233339]
65. Lymn RW, Taylor EW. Mechanism of adenosine triphosphate hydrolysis by actomyosin. Biochemistry. 1971; 10(25):4617–24. [PubMed: 4258719]
66. Tyska MJ, Warshaw DM. The myosin power stroke. Cell Motil Cytoskeleton. 2002; 51(1):1–15. [PubMed: 11810692]
67. Tanner BC, et al. Kinetics of cardiac myosin isoforms in mouse myocardium are affected differently by presence of myosin binding protein-C. J Muscle Res Cell Motil. 2014; 35(5–6):267–78. [PubMed: 25287107]
68. Wang Y, et al. Cardiac myosin isoforms exhibit differential rates of MgADP release and MgATP binding detected by myocardial viscoelasticity. J Mol Cell Cardiol. 2013; 54:1–8. [PubMed: 23123290]
69. Pulcastro HC, et al. Effects of myosin light chain phosphorylation on length-dependent myosin kinetics in skinned rat myocardium. Archives of Biochemistry and Biophysics.
70. Dobesh DP, Konhilas JP, de Tombe PP. Cooperative activation in cardiac muscle: impact of sarcomere length. American Journal of Physiology - Heart and Circulatory Physiology. 2002; 282(3):H1055–H1062. [PubMed: 11834504]
71. Kentish JC, et al. Comparison between the sarcomere length-force relations of intact and skinned trabeculae from rat right ventricle. Influence of calcium concentrations on these relations. Circulation Research. 1986; 58(6):755–68. [PubMed: 3719928]
72. Beer, ELd, et al. Effect of sarcomere length and filament lattice spacing on force development in skinned cardiac and skeletal muscle preparations from the rabbit. Basic Research in Cardiology. 1988; 83(4):410–423. [PubMed: 3190659]
73. Farman GP, et al. The role of thin filament cooperativity in cardiac length-dependent calcium activation. Biophys. J. 2010; 99(9):2978–2986. [PubMed: 21044595]
74. Fuchs F, Martyn DA. Length-dependent Ca(2+) activation in cardiac muscle: some remaining questions. J Muscle Res Cell Motil. 2005; 26(4–5):199–212. [PubMed: 16205841]
75. Geeves MA, Lehrer SS. Cross-talk, cross-bridges, and calcium activation of cardiac contraction. Biophys J. 2014; 107(3):543–5. [PubMed: 25099792]
76. Loong CKP, Badr MA, Chase PB. Tropomyosin Flexural Rigidity and Single Ca(2+) Regulatory Unit Dynamics: Implications for Cooperative Regulation of Cardiac Muscle Contraction and Cardiomyocyte Hypertrophy. Frontiers in Physiology. 2012; 3:80. [PubMed: 22493584]
77. Sun Y-B, Irving M. The molecular basis of the steep force-calcium relation in heart muscle. Journal of Molecular and Cellular Cardiology. 2010; 48(5):859–865. [PubMed: 20004664]
78. Land S, Niederer SA. A Spatially Detailed Model of Isometric Contraction Based on Competitive Binding of Troponin I Explains Cooperative Interactions between Tropomyosin and Crossbridges. PLoS Comput Biol. 2015; 11(8):e1004376. [PubMed: 26262582]

Author Manuscript Author Manuscript Author Manuscript Author Manuscript

79. Terui T, et al. Regulatory mechanism of length-dependent activation in skinned porcine ventricular muscle: role of thin filament cooperative activation in the Frank-Starling relation. The Journal of General Physiology. 2010; 136(4):469. [PubMed: 20876361]

80. Kobayashi T, Jin L, de Tombe PP. Cardiac thin filament regulation. Pflugers Arch. 2008; on-line. doi: 10.1007/s00424-008-0511-8

81. Tachampa K, et al. Increased Cross-bridge Cycling Kinetics after Exchange of C-terminal Truncated Troponin I in Skinned Rat Cardiac Muscle. The Journal of Biological Chemistry. 2008; 283(22):15114–15121. [PubMed: 18378675]

82. Metskas LA, Rhoades E. Order-Disorder Transitions in the Cardiac Troponin Complex. J Mol Biol. 2016; 428(15):2965–77. [PubMed: 27395017]

83. Gao WD, Dai T, Nyhan D. Increased cross-bridge cycling rate in stunned myocardium. American Journal of Physiology - Heart and Circulatory Physiology. 2006; 290(2):H886–H893. [PubMed: 16172165]

84. Yang C, et al. The Influence of Myosin Converter and Relay Domains on Cross-Bridge Kinetics of Drosophila Indirect Flight Muscle. Biophysical Journal. 2010; 99(5):1546–1555. [PubMed: 20816067]

85. Foster DB, et al. C-terminal truncation of cardiac troponin I causes divergent effects on ATPase and force: implications for the pathophysiology of myocardial stunning. Circ Res. 2003; 93(10): 917–24. [PubMed: 14551240]

Author Manuscript Author Manuscript Author Manuscript Author Manuscript

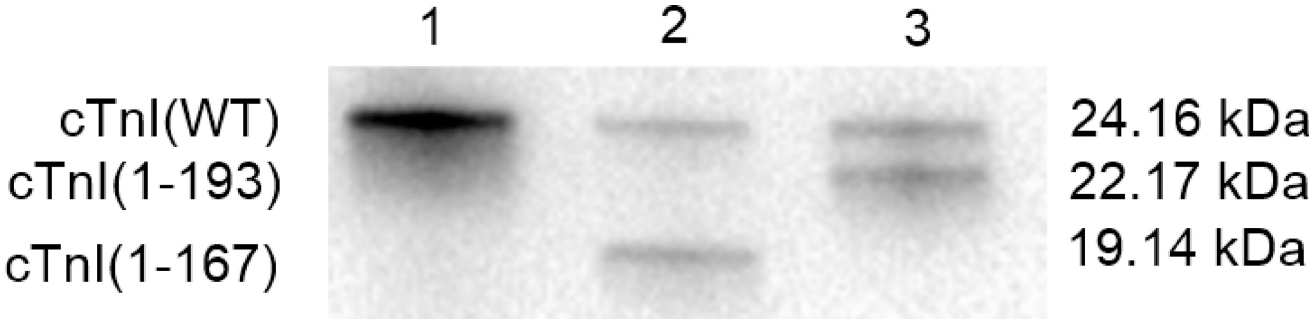

Figure 1.

Western blot analysis of reconstituted cardiac muscle preparations. Anti cTnI antibody was used to assess the level of the incorporation of cTnI-MD truncations into the reconstituted cardiac muscle preparations. Starting from the left, lanes 1, 2, and 3 shows cTnI(WT), cTnI(1–167), and cTnI(1–193) reconstituted cardiac muscle fibers, respectively. Image J software was used for densitometric analysis of band intensities and the relative amount of incorporated cTnI(1–167) and cTnI(1–193) was 64% ± 5 (n=3) for both.

Author Manuscript Author Manuscript Author Manuscript Author Manuscript

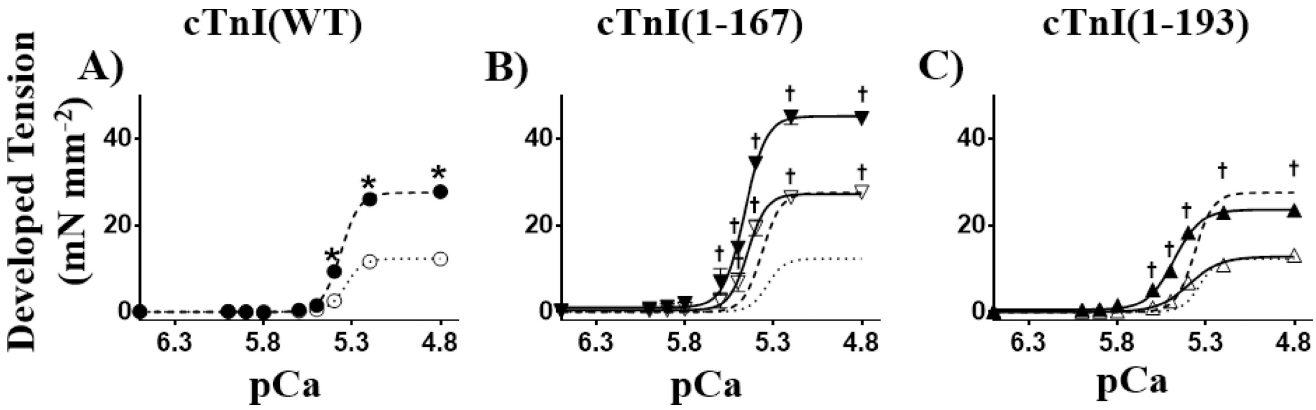

Figure 2.

cTnI-MD truncations affected the tension-pCa relationship differently at long vs. short SL. Developed tension-pCa relationships for A) cTnI(WT) (●) and (○) at 2.2 and 1.9μm SLs, respectively; B) cTnI(1–167) (▼) and (▽) at 2.2 and 1.9μm SLs, respectively; and C) cTnI(1–193) (▲) and (Δ) at 2.2 and 1.9μm SLs, respectively. Lines represent 3-parameter Hill fits to the tension-pCa data, with the fine dashed line representing cTnI(WT) fit at 1.9μm SL, and bold dashed line for cTnI(WT) fit at 2.2μm SL replotted in panel B and C.

*: SL effect for cTnI(WT); $P < 0.05$

†: Truncation effect compared to cTnI(WT) at same SL; $P < 0.05$

Author Manuscript Author Manuscript Author Manuscript Author Manuscript

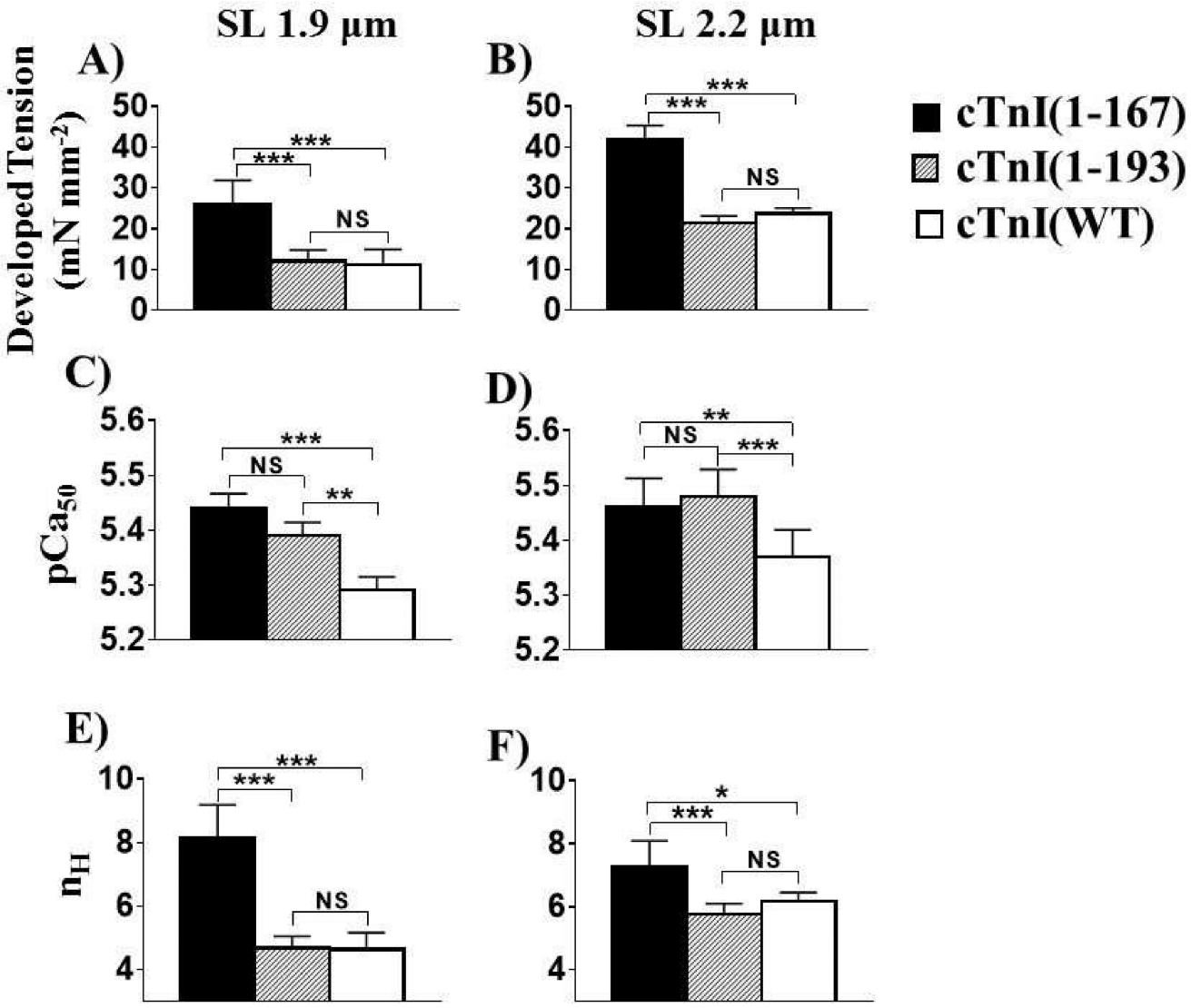

Figure 3.

cTnI-MD truncations sensitize the muscle to Ca^{2+} at both short and long SLs. Developed tension, pCa_{50} and n_H (A, C, and E for short SL and B, D, and F for long SL) for cTnI(WT), cTnI(1–167), and cTnI(1–193) exchanged skinned fibers were plotted at each SL.

*: truncation effect at same SL; $P < 0.05$, based on two-way ANOVA results.

NS: not statistically significant.

Author Manuscript
Author Manuscript
Author Manuscript
Author Manuscript

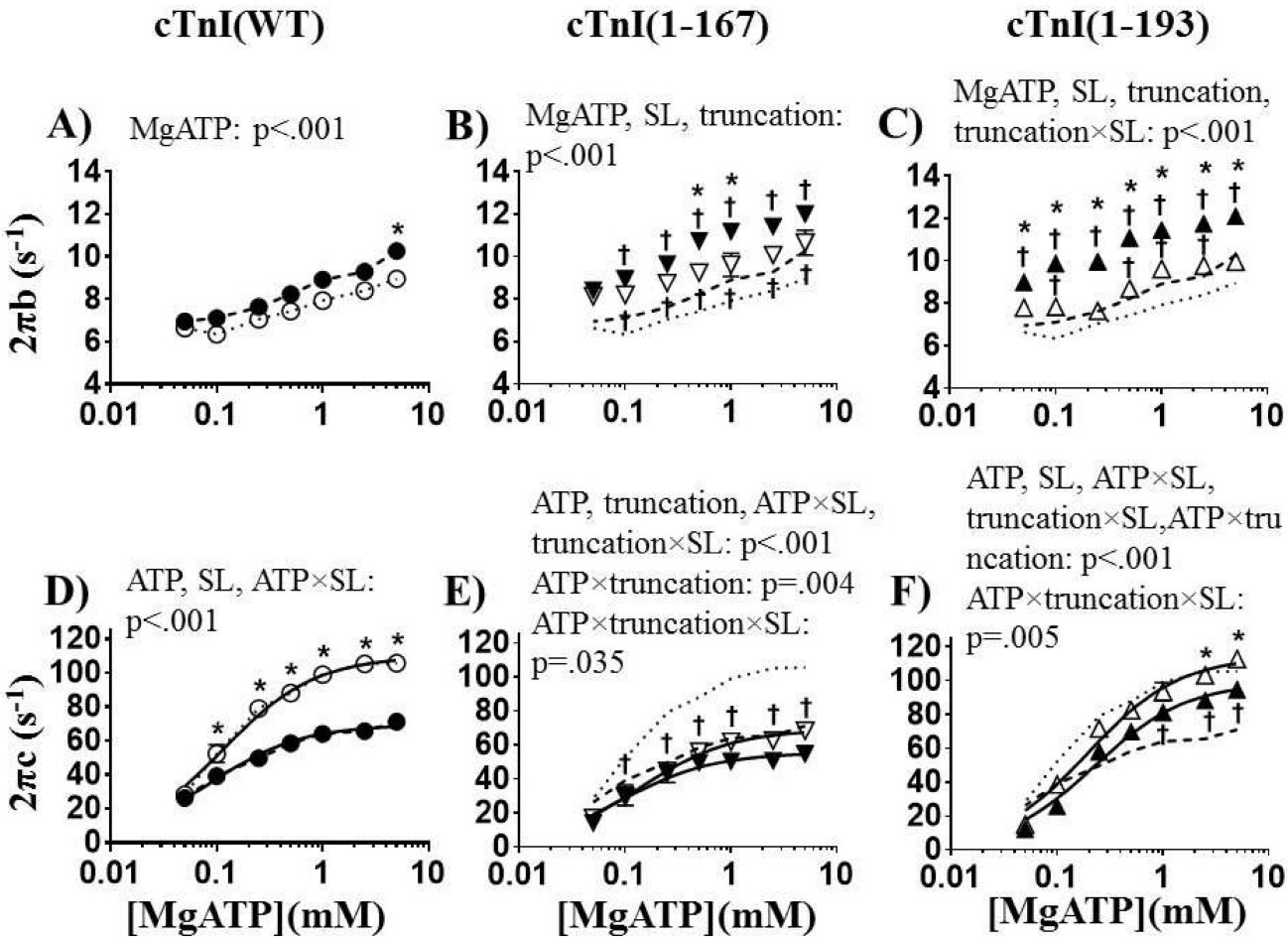

Figure 4.

cTnI-MD truncations influenced cross-bridge kinetics as [MgATP] varied at pCa 4.8. Cross-bridge attachment rates (2πb) and cross-bridge detachment rates (2πc) are plotted against [MgATP] for A and D) cTnI(WT) (●) and (○) at 2.2 and 1.9μm SLs, respectively; B and E) cTnI(1–167) (▼) and (▽) at 2.2 and 1.9μm SLs, respectively; and C and F) cTnI(1–193) (▲) and (Δ) at 2.2 and 1.9μm SLs, respectively. Solid lines at 2πc (D, E, and F panels) represents fitting 2πc-[MgATP] relationship to Eq. (2) to extract the model parameters explaining nucleotide handling rates. The fine dashed line represents the cTnI(WT) at short SL, and bold dashed line represents cTnI(WT) at long SL replotted on the middle and right panels for easy comparison.

*: SL effect for each truncation or wild-type fibers; $P < 0.05$

†: truncation effect compared to cTnI(WT); $P < 0.05$

Author Manuscript Author Manuscript Author Manuscript Author Manuscript

Arch Biochem Biophys. Author manuscript; available in PMC 2018 November 15.

Table 1

Characteristics of tension-pCa relationships in rat myocardium at 1.9 and 2.2μm SLs, for cTnI(WT), cTnI(1–167), and cTnI(1–193) fibers (Mean± SEM)

	cTnI(WT)		cTnI(1–167)		cTnI(1–193)	
	1.9μm	**2.2μm**	**1.9μm**	**2.2μm**	**1.9μm**	**2.2μm**
T_{min} (mN mm^{-2})	1.00±0.06	3.74±0.26*	1.24±0.19	3.34±0.09*	0.67±0.03	2.15±0.29$^{*\dagger\#}$
T_{max} (mN mm^{-2})	13.25±1.75	31.25±0.62*	28.42±1.59†	47.96±1.37*†	13.38±1.07$^{\#}$	25.72±0.73$^{*\#}$
T_{dev} (mN mm^{-2})	12.25±1.50	27.51±0.54*	27.18±2.21†	44.62±1.29*†	12. 71±1.1$^{\#}$	23.5 7±0.69$^{*\#}$
pCa_{50}	5.29±0.01	5.37±0.02*	5.44±0.01†	5.46±0.02†	5.39±0.01$^{\dagger\#}$	5.48±0.02*†
n_H	4.64±0.21	6.18±0.11*	8.15±0.39†	7.27±0.21†	4.68±0.15$^{\#}$	5.78±0.13$^{*\#}$
n fibers	6	6	7	7	6	6

T_{min}, absolute tension value at pCa 8.0; T_{max}, absolute tension value at pCa 4.8; T_{dev}, Ca^{2+}-activated developed tension (T_{max}- T_{min}); pCa_{50} and n_H represent fit parameters to a 3-parameter Hill equation.

*Effect of SL for each truncation or wild-type; $P<0.05$

†Truncation effect compared to cTnI(WT) at same SL; $P<0.05$

$^{\#}$Difference between cTnI(1–193) and cTnI(1–167) at same SL; $P<0.05$

Author Manuscript Author Manuscript Author Manuscript Author Manuscript

Table 2

Estimates of myosin nucleotide handling rates from fits of the cross-bridge detachment rate (2πc) vs. [MgATP] relationships to Eq. (2) for cTnI(WT) and cTnI-MD truncations at 1.9 and 2.2μm SLs (mean ± SEM).

	cTnI(WT)		cTnI(1–167)		cTnI(1–193)	
	1.9μm	**2.2μm**	**1.9μm**	**2.2μm**	**1.9μm**	**2.2μm**
k_{-ADP} (S^{-1})	109.8±1.96	74.01±1.75 *	69.1±1.96 †	55.51±2.66 *†	114.6±3.25 #	99.15±2.13 *†#
K_{+ATP} (mM^{-1} S^{-1})	950.6±69.17	813.8±68.56	506.9±55.84 †	589.9±122.3	585.5±57.98 †	437.2±3 1.36 †
n fibers	6	6	7	7	6	6

k_{-ADP}, cross-bridge MgADP release rate; k_{+ATP}, cross-bridge MgATP binding rate

* Effect of SL for each truncation or wild-type; $P<0.05$

† Truncation effect compared to cTnI(WT) at same SL; $P<0.05$

Difference between cTnI(1–193) and cTnI(1–167) at same SL; $P<0.05$